NONCOHERENT DEMODULATOR FOR PPM-UWB RADIOS

Liuqing Yang[1] *and* *Ananthram Swami*[2]

[1]Dept. of ECE, Univ. of Florida, P.O. Box 116130, Gainesville, FL 32611
[2]Army Research Lab, 2800 Powder Mill Road, Adelphi, MD 20783

ABSTRACT

Low-duty-cycle Ultra-wideband (UWB) radios have the potential to provide low-probability of detection (LPD) communications with low-power and low-complexity implementation. Pulse position modulation (PPM) is a prevalent scheme for UWB radios since it can further lower the transmitter complexity by avoiding pulse negation. However, the position shifts of impulse-like UWB waveforms, together with the severe frequency-selectivity of the propagation channels, aggravate the difficulty and complexity of timing synchronization and channel estimation. To circumvent both of these challenging tasks, we develop a differential encoder and its corresponding noncoherent demodulator for PPM-UWB signals. Relying on integrate-and-dump operations of "dirty" templates, our designs are operational when the timing offset and channel information both remain unknown.

1. INTRODUCTION

To realize the unique benefits of ultra-wideband (UWB) transmissions, timing synchronization and channel estimation pose two preeminent challenges, which have spurred extensive research in these areas. As a result of these efforts, timing acquisition algorithms have been derived to provide reasonable performance even in the presence of *unknown* multipath channel [1, 10, 12]. Nevertheless, timing errors are inevitable, especially under low complexity constraints. In the last few years, UWB receivers circumventing channel estimation have also been developed, which include the transmitted reference (TR) scheme[1] and a differential approach (see e.g., [4, 5, 6]). Such approaches, though obviating the need for explicit UWB channel estimation, still require accurate timing.

Recently, optimum and suboptimum fully noncoherent demodulators were developed and simulated in [15]. These demodulators remain operational even when timing and channel estimation are both bypassed. Apparently, as existing differential approaches, these noncoherent demodulators are only applicable to pulse amplitude modulated (PAM-)UWB signals.

Being able to avoid pulse negation, pulse position modulation (PPM) can lower the implementation complexity and is particularly suitable for UWB transmissions[2] [8, 14]. However, the PPM-induced position shifts of impulse-like UWB waveforms, together with the severe frequency-selectivity of the propagation channels, aggravate the difficulty and complexity of timing synchronization and channel estimation. These render differential and/or noncoherent schemes more desirable. However, no such schemes have been investigated.

Inspired by the PPM-UWB timing algorithm recently established in [12], we develop here a novel noncoherent demodulator for nonlinearly modulated PPM-UWB signals. As in [12], our approach is built on the correlation between neighboring modified "dirty" templates. But instead of attempting to estimate the timing offset, we utilize the symbol-rate correlator outputs to form symbol estimates directly. When timing information is not available, or when timing error is present, our demodulator operates in the noncoherent mode *without* either timing or channel knowledge. When perfect timing is achieved, our demodulator operates in the differential (a.k.a. semi-coherent) mode in the sense that channel estimation is bypassed.

Our objective and the approach of correlating noisy received waveform are inspired by those in [15] for PAM-UWB signals. However, the nature of the PPM modulation renders the original "dirty" templates deployed in [14, 15] unusable. This motivates us to resort to the *modified* "dirty" templates by utilizing the PPM modulation index known to the receiver. To enable a noncoherent demodulator, we develop a differential encoding scheme that is tailored for PPM modulations, and come up with novel receiver processing to allow the (quasi-)optimum adoption of a maximum-likelihood sequence detector (MLSD) in the form of Viterbi's algorithm. All these make our system design suitable for PPM-UWB signals, and thus distinct from existing ones developed for PAM-UWB.

2. SYSTEM MODEL AND PROBLEM STATEMENT

In typical low-duty-cycle UWB radios, every information symbol is conveyed by N_f pulses $p(t)$ each with duration T_p. During each frame of duration $T_f > T_p$, one data-modulated $p(t)$ is transmitted. The resultant symbol duration is $T_s = N_f T_f$ seconds. In order to accommodate multiple users, pseudo-random time-hopping (TH) and/or direct-sequence (DS) spreading codes are often employed [7, 8, 14]. Unlike DS codes that modify the polarity of individual pulses, TH codes shift the pulse positions from frame to frame at multiples of the chip duration $T_c := \lfloor T_f/N_c \rfloor$, where N_c denotes the number of chips per frame. These spreading codes can also serve the purpose of smoothing the transmit spectrum as well as providing low probability of detection (LPD). The two prevalent modulation schemes in UWB impulse radios are PAM and PPM. Between the two, PPM renders pulse negation unnecessary and can reduce the implementation complexity. Here we consider binary PPM modulation where symbol '0' is represented by $p(t)$ and symbol '1' is represented by $p(t-\Delta)$ with Δ being the modulation index. The transmitted signal is then given by:

$$v(t) = \sqrt{\mathcal{E}} \sum_{n=0}^{+\infty} \sum_{k=0}^{N_f-1} c_k^{ds} \cdot p(t - nT_s - kT_f - c_k^{th} T_c - \tilde{s}_n \Delta), \qquad (1)$$

where $\mathcal{E}$ is the transmit energy per pulse, $\tilde{s}_n$ is the nth differentially encoded symbol, and c_k^{ds} and c_k^{th} are the symbol-periodic DS and TH codes during the kth frame, respectively. We allow the TH code to take any integer value in the range $[0, N_c - 1]$. Notice that this can give rise to (at times considerable) inter-frame interference (IFI).

Differential encoding has been extensively investigated for both narrowband and ultra-wideband systems [5, 15], but is only applicable to linear modulations such as PSK and PAM. Here, we develop a differential encoding scheme tailored for PPM-UWB:

$$\tilde{s}_n = s_n \oplus \tilde{s}_{n-1} ,$$

where $s_n \in \{0, 1\}$ is the nth original information symbol, $\tilde{s}_{n-1}$ is the $(n-1)$st differentially encoded symbol, and $\oplus$ denotes the modulo-2 summation. In the ensuing section, we will show that such

[1]Optimized versions of TR ameliorating its 50% rate or energy loss are also available [13, 16].

[2]Compared to the antipodal PAM modulation, PPM comes with a BER degradation for a fixed signal-to-noise ratio (SNR).

1-4244-0469-X/06/$20.00 ©2006 IEEE

Table 1.

$\{s_m, s_{m+1}\}$	$\{\tilde{s}_{m-1}, \tilde{s}_m, \tilde{s}_{m+1}\}$	$\{\check{s}_m, \check{s}_{m+1}\}$
$\{0,0\}$	$\{0,0,0\}$	$\{0,0\}$
$\{0,1\}$	$\{0,0,1\}$	$\{0,-1\}$
$\{1,0\}$	$\{0,1,1\}$	$\{-1,0\}$
$\{1,1\}$	$\{0,1,0\}$	$\{-1,1\}$
$\{0,0\}$	$\{1,1,1\}$	$\{0,0\}$
$\{0,1\}$	$\{1,1,0\}$	$\{0,1\}$
$\{1,0\}$	$\{1,0,0\}$	$\{1,0\}$
$\{1,1\}$	$\{1,0,1\}$	$\{1,-1\}$

a differential encoding scheme enables detection of PPM symbols at the receiver without either timing or channel information.

Denoting the transmitted symbol-level waveform $p_T(t)$ containing N_f pulses as $p_T(t) := \sum_{k=0}^{N_f-1} c_k^{ds} \cdot p(t - kT_f - c_k^{th} T_c)$, Eq. (1) becomes:

$$v(t) = \sqrt{\mathcal{E}} \sum_{n=0}^{+\infty} p_T(t - nT_s - \tilde{s}_n \Delta).$$

Our notion of differential PPM is different from that in the optical communications literature, e.g., [9, 17].

We model the quasi-static multipath channel as a tapped-delay line, with $(L+1)$ taps $\{\alpha_l\}_{l=0}^{L}$ and delays $\{\tau_l\}_{l=0}^{L}$, which remain invariant over one transmission burst but are allowed to change across bursts. Focusing on a peer-to-peer link, the waveform arriving at the receiver is given by:

$$r(t) = \sqrt{\mathcal{E}} \sum_{n=0}^{+\infty} p_R(t - nT_s - \tilde{s}_n \Delta - \tau_0) + \eta(t) \;, \qquad (2)$$

where the noise term $\eta(t)$ includes additive white Gaussian noise (AWGN) as well as multiuser interference,

$$p_R(t) := \sum_{l=0}^{L} \alpha_l p_T(t - \tau_{l,0}) \qquad (3)$$

is the aggregate channel capturing both the pulse shaper, TH/DS spreading and the multipath effects, and $\tau_{l,0} := \tau_l - \tau_0$ denotes the lth path delay isolated from the propagation delay τ_0.

To establish our noncoherent UWB (de)modulation, we will select $T_f \geq \tau_{L,0} + T_p + \Delta$ and $c_0^{th} \geq c_{N_f-1}^{th}$ in order to confine the duration of $p_R(t)$ within $[0, T_s)$, and avoid inter-symbol interference (ISI). It is worth emphasizing that we allow IFI to be present even when ISI is avoided. In fact, since our demodulation algorithm only requires zero ISI, the condition $T_f \geq \tau_{L,0} + T_p + \Delta$ can certainly be relaxed to allow for higher data rates, as long as guard frames are inserted between symbols to avoid ISI, much like zero-padding in narrowband systems. Without loss of generality, we also confine the timing offset τ_0 within a symbol duration; i.e., $\tau_0 \in [0, T_s)$.

3. NONCOHERENT PPM-UWB DEMODULATOR

Starting from the noisy received waveform $r(t)$ with *unknown* timing offset τ_0 and unknown waveform $p_R(t)$ in (2), we will develop our optimum noncoherent demodulation algorithm in three steps: extraction of dirty templates, an integrate and dump operation, followed by demodulation.

3.1. Step 1: Form "Dirty" Templates

The first step follows that in the noncoherent approach for PAM-UWB signals in [15]. We consider a burst of duration MT_s, and extract segments of duration T_s, yielding

$$r_m(t) = r(t + mT_s), \;\; t \in [0, T_s), \;\; m \in [0, M-1]. \qquad (4)$$

Substituting (2) into (4), we have:

$$r_m(t) = \sqrt{\mathcal{E}}\, p_R(t + T_s - \tau_0 - \tilde{s}_{m-1}\Delta) + \sqrt{\mathcal{E}}\, p_R(t - \tau_0 - \tilde{s}_m \Delta) + \eta_m(t),$$

where $\eta_m(t) := \eta(t + mT_s)$, $\forall t \in [0, T_s)$. Notice that, due to the timing offset τ_0, $r_m(t)$ involves two adjacent symbols.

These symbol-long received segments $r_m(t)$ are "dirty" in several senses: they are not only noisy, but also delayed by the *unknown* timing offset τ_0 as well as distorted by the *unknown* propagation channel. Notice that these differ from the noisy and distorted templates used in TR and differential UWB, which are taken at the correct time instances (i.e., $\tau_0 = 0$).

When PAM is deployed, $r_m(t)$ and $r_{m+1}(t)$ can be directly used as the "dirty" templates at the receiver correlator. However, for PPM-UWB signals, this approach is not feasible simply because the information symbols are embedded in the relative delay of the aggregate waveforms $p_R(t)$, as opposed to the *linear* multiplicative polarity change when PAM is used. Inspired by the timing acquisition approach recently developed in [12] for PPM-UWB signals, we use $r_{m+1}(t)$ as one of the "dirty" templates at the correlator and form the other as follows:

$$\tilde{r}_m(t) := r(t + mT_s + \Delta) - r(t + mT_s - \Delta), \; t \in [0, T_s). \qquad (5)$$

Intuitively, this modified dirty template relies on the fact that, with binary PPM, one of the shifted (by $\pm\Delta$) versions of $r_m(t)$ will be aligned with $r_{m+1}(t)$. Next, we will show that *noncoherent* PPM symbol demodulation is possible with such generated "dirty" templates, obviating the need for timing and channel estimation.

3.2. Step 2: Integrate-and-Dump

Upon extracting these "dirty" templates, the second step of our noncoherent demodulation algorithm amounts to correlating $\tilde{r}_m(t)$ with $r_{m+1}(t)$. This operation results in symbol-rate samples

$$x(m) := \int_0^{T_s} \tilde{r}_m(t) r_{m+1}(t) dt. \qquad (6)$$

Along the lines of [12, Lemma 1], Eq. (6) can be simplified to:

$$x(m) = (\tilde{s}_{m-1} - \tilde{s}_m)\mathcal{E}_A + (\tilde{s}_m - \tilde{s}_{m+1})\mathcal{E}_B + \zeta(m) \;, \qquad (7)$$

where $\mathcal{E}_A := \mathcal{E} \int_0^{T_s} p_R^2(t + T_s - \tau_0) dt = \mathcal{E} \int_{T_s - \tau_0}^{T_s} p_R^2(t) dt$ and $\mathcal{E}_B := \mathcal{E} \int_0^{T_s} p_R^2(t - \tau_0) dt = \mathcal{E} \int_0^{T_s - \tau_0} p_R^2(t) dt = \mathcal{E}_R - \mathcal{E}_A$ with $\mathcal{E}_R := \mathcal{E} \int_0^{T_s} p_R^2(t) dt$ capturing the entire energy of the aggregate channel in (3). Notice that the information originally conveyed in the pulse positions is now converted into *linear* multiplicative polarity changes, thanks to the careful construction of template $\tilde{r}_m(t)$.

If perfect timing is achieved (i.e., $\tau_0 = 0$), then one has $\mathcal{E}_A = 0$, $\mathcal{E}_B = \mathcal{E}_R$ and (7) boils down to $x(m) = (\tilde{s}_m - \tilde{s}_{m+1})\mathcal{E}_R + \zeta(m)$, where $(\tilde{s}_m - \tilde{s}_{m+1}) \in \{-1, 0, +1\}$ can be readily demodulated. This brief exposition implies that even with PPM modulation, differential encoding and decoding is still possible, provided that the modulation index Δ is exploited by the dirty template formulation. This differential PPM-UWB system is a nice complement to existing research on differential UWB systems (see e.g., [5]), which focus on linear PAM modulated signals.

However, such a differential UWB receiver is only semi-coherent: although it bypasses channel estimation, perfect timing is still required. In reality, even when synchronization is attempted with various approaches such as [1, 10, 12], timing errors are inevitable and thus $\tau_0 \neq 0$, especially when complexity is of concern. In such cases, $\mathcal{E}_A$ and $\mathcal{E}_B$ are both nonzero. As a result, direct application of differential demodulation will lead to considerable performance loss. This motivates our fully noncoherent UWB demodulation algorithms that not only circumvents channel estimation, but also account for the *unknown* timing offset, or equivalently, timing error

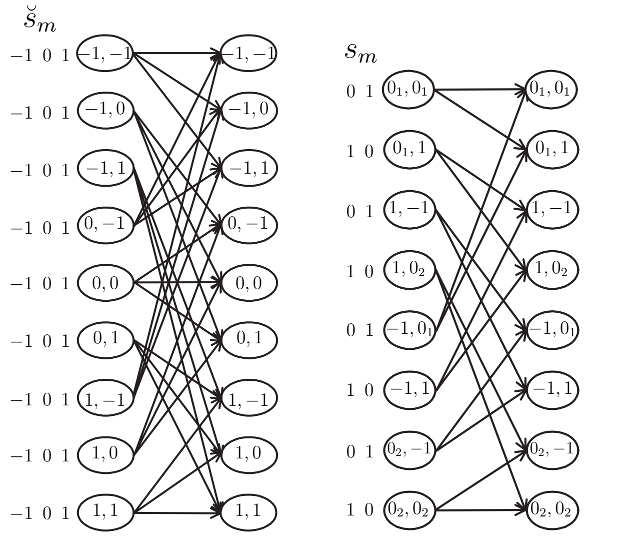

(a) (b)

Fig. 1. (a) Trellis for the suboptimum MLSD in (9); and (b) Trellis for the optimum noncoherent MLSD.

τ_0. Before deriving such algorithms, let us first investigate the noise term $\zeta(m)$ in (7).

It can be shown that the noise $\zeta(m)$ is the superposition of the following three components:

$$\zeta_1(m) := \int_0^{T_s} \tilde{\rho}_m(t)\eta_{m+1}(t)dt$$

$$\zeta_2(m) := \int_0^{T_s} \rho_{m+1}(t)(\eta_m(t+\Delta) - \eta_m(t-\Delta))dt$$

$$\zeta_3(m) := \int_0^{T_s} \eta_{m+1}(t)(\eta_m(t+\Delta) - \eta_m(t-\Delta))dt$$

where $\tilde{\rho}_k(t;\tau) = \sqrt{\mathcal{E}}\,[\tilde{p}_R(t+T_s-\tau_0-s_{k-1}\Delta)+\tilde{p}_R(t-\tau_0-s_k\Delta)]$ and $\tilde{p}_R(t-s_k\Delta) := p_R(t-s_k\Delta+\Delta)-p_R(t-s_k\Delta-\Delta)$.

These components are similar to the noise terms one finds in TR or Pilot Waveform Assisted Modulation (PWAM) as well as in differential and noncoherent UWB systems [2, 5, 6, 16]. With $\eta(t)$ in (2) being bandpass filtered AWGN with zero mean and double-sided power spectral density $\sigma^2/2$, straightforward extension of the results in [12] reveals that the double noise term $\zeta_3(m)$ can be approximated as Gaussian variables with zero mean, and is uncorrelated with $\zeta_1(m)$ and $\zeta_2(m)$. It then follows that the overall noise $\zeta(m)$ in the symbol-rate sample $x(m)$ is also zero-mean Gaussian with variance $\sigma_\zeta^2 := 2\mathcal{E}_R N_0 + N_0^2 B T_s$, where B is the double-sided bandwidth of the receiver's front-end.

3.3. Step 3: Quasi-ML Demodulator

Upon defining $\breve{s}_m := \tilde{s}_{m-1} - \tilde{s}_m$, Eq. (7) can be simplified to:

$$x(m) = \breve{s}_m \cdot \mathcal{E}_A + \breve{s}_{m+1} \cdot \mathcal{E}_B + \zeta(m), \tag{8}$$

where $\breve{s}_m$ is related to the original symbols s_m by the relationship: $s_m = [\breve{s}_m]_{\text{mod}2}$. Since $\tau_0 \neq 0$ in general, each correlator output $x(m)$ involves two successive symbols, namely $\breve{s}(m)$ and $\breve{s}(m+1)$. As a result, $\{x(m)\}$ can be viewed as symbol-rate samples of an unknown first-order ISI channel, whose impulse response taps are nothing but the partial channel energies $\mathcal{E}_A$ and $\mathcal{E}_B$ in (8). These interesting points lead to noncoherent algorithms for joint symbol detection and estimation of the unknown equivalent channel based on the "dirty correlator" output samples in (8). It is worth emphasizing that only two equivalent channel taps are to be estimated with our noncoherent UWB setup, as opposed to hundreds of taps in the underlying UWB physical channel. Recall that the symbol rate samples are obtained via the analog correlator of (2) which involves at most two fixed tapped delay lines (see (5)).

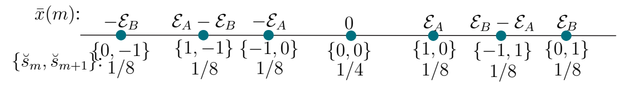

Fig. 2. An example of the constellation points of $\bar{x}(m)$ with different $\{\breve{s}_m, \breve{s}_{m+1}\}$ values.

With the ISI channel model in (8), the demodulator is seemingly straightforward, using an MLSD. Consider one sample $x(m)$ that consists of only two symbols $\breve{s}_m$ and $\breve{s}_{m+1}$. With the differentially encoded symbols $\tilde{s}_m \in \{0, 1\}$, $\breve{s}_m$ can take 3 possible values $\{-1, 0, +1\}$. Hence, the following minimum distance metric can be used for each MLSD evolution:

$$|\breve{s}_m \mathcal{E}_a + \breve{s}_{m+1}\mathcal{E}_B - x(m)|^2, \ \ \forall \breve{s}_m, \breve{s}_{m+1} \in \{-1, 0, +1\}\ . \tag{9}$$

Such an MLSD can be implemented by Viterbi's algorithm (VA), which entails comparing 3 incoming paths at each of the $3^2 = 9$ possible states, as depicted in Fig. 1(a).

However, a closer look at the model in (8) will reveal that the MLSD in (9) is suboptimum and overly complicated. The values of the sequence $\{\breve{s}_m, \breve{s}_{m+1}\}$ corresponding to all possible information symbol sequences are listed in Table 1. Notice that out of the total of 9 possible $\{\breve{s}_m, \breve{s}_{m+1}\}$ pairs, only 7 made appearance in Table 1, and with *unequal* probabilities. We then found that the optimum MLSD relies on the trellis as shown in Fig. 1(b). Its corresponding VA entails comparing 2 incoming paths at each of the 8 possible states and reduces the complexity of (9) by nearly 50%.

Clearly, the implementation of the symbol detection heavily hinges upon the estimation of the partial channel energies $\mathcal{E}_A$ and $\mathcal{E}_B$. Since the MLSD is optimum only with the perfect knowledge of $\mathcal{E}_A$ and $\mathcal{E}_B$, we hence term our demodulator quasi-ML. At first glance, $\mathcal{E}_A$ and $\mathcal{E}_B$ rely on both the channel information and the timing acquisition. However, we will show next that, without timing synchronization and channel estimation, $\mathcal{E}_A$ and $\mathcal{E}_B$ can be estimated from the symbol-rate samples $x(m)$ only. Let $\bar{x}(m)$ represent the noise-free part of $x(m)$. The constellation points of $\bar{x}(m)$ together with their probabilities of occurrence are also visualized in Fig. 2. This figure indicates that $|\bar{x}(m)|$ can only take four values. In fact, we can prove that $\{|\bar{x}(m)|\}$ are as i.i.d. random variables, with mean and mean-square:

$$\begin{aligned} \mathrm{E}\{|\bar{x}(m)|\} &= \mathcal{E}_{\max}/2 \\ \mathrm{E}\{|\bar{x}(m)|^2\} &= [\mathcal{E}_{\min}^2 + \mathcal{E}_{\max}^2 + (\mathcal{E}_{\max} - \mathcal{E}_{\min})^2]/4 \end{aligned} \tag{10}$$

where $\mathcal{E}_{\max} := \max\{\mathcal{E}_A, \mathcal{E}_B\}$ and $\mathcal{E}_{\min} := \min\{\mathcal{E}_A, \mathcal{E}_B\}$. Solving (10) and replacing the ensemble mean with the sample mean then give rise to the estimates $\hat{\mathcal{E}}_{\max}$ and $\hat{\mathcal{E}}_{\min}$. In order to obtain $\hat{\mathcal{E}}_A$ and $\hat{\mathcal{E}}_B$ from $\hat{\mathcal{E}}_{\max}$ and $\hat{\mathcal{E}}_{\min}$, we need an initial value to determine their relative magnitudes. To this end, two known symbols can be transmitted at the beginning of every burst, as in [15].

3.4. Quasi-ML Noncoherent UWB Demodulation

Over a burst of duration MT_s, our quasi-optimum noncoherent demodulator operates as follows:

- S1. Take symbol-long segments of the received waveform $r_m(t)$ as in (4), $\forall m \in [0, M-1]$.
- S2. Form the modified "dirty" templates $\tilde{r}_m(t)$ as in (5), $\forall m \in [0, M-1]$.
- S3. Integrate-and-dump the product of neighboring (modified) dirty templates $\tilde{r}_m(t)$ and $r_{m+1}(t)$, to obtain $x(m)$, $\forall m \in [0, M-1]$, as in (6).
- S4. Form estimates $\hat{\mathcal{E}}_A$ and $\hat{\mathcal{E}}_B$.

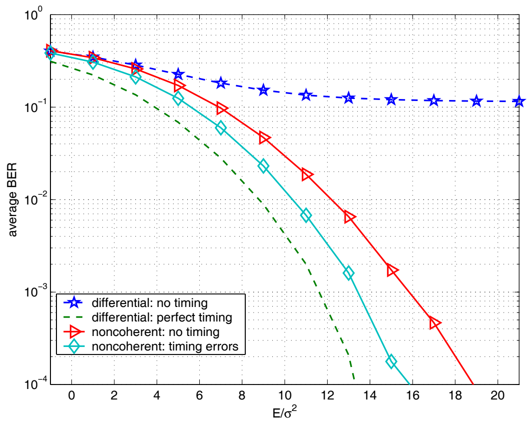

Fig. 3. BER comparison between differential and noncoherent PPM-UWB signaling, with no timing efforts, when the timing is perfect, and in the presence of residual timing errors.

S5. Demodulate using MLSD such as VA, or trading-off performance for complexity, with its per-survivor variants.

4. SIMULATIONS

In this section, simulations will be performed to compare the average bit-error-rate (BER) performance of our noncoherent demodulation algorithm with the differential approach for PPM-UWB signals. Unlike the noncoherent demodulation that accounts for the timing offset or residual timing errors, the differential approach is a semi-coherent approach that bypasses channel estimation but require timing information. With the latter, the received signal is demodulated assuming that perfect timing is achieved. Coherent symbol demodulation is also possible via e.g., Rake reception after timing and channel estimation [11]. Considering demodulators with similar complexity, we will focus on comparisons between noncoherent and semi-coherent demodulators.

The pulse shaper $p(t)$ used in our simulations is a Gaussian monocycle with duration $T_p = 1.0$ns. The number of frames per symbol is $N_f = 32$. The frame duration is chosen to be $T_f = 35$ns to avoid ISI. The multipath channels are generated using the CM1 channel model in [3] with real channel taps and parameters $(1/\Lambda, 1/\lambda, \Gamma, \gamma) = (43, 0.4, 7.1, 4.3)$ns. The TH codes are generated independently from a uniform distribution over $[0, N_c - 1]$ with $N_c = 17$ and $T_c = 2$ns. Timing offsets τ_0 are uniformly distributed over $[0, T_s)$. When timing synchronization is also performed, the "dirty" template based acquisition algorithm of [12] is used with 4 training symbols, 2 out of which can also be used in the estimation of $\mathcal{E}_A$ and $\mathcal{E}_B$.

Fig. 3 depicts the average BER of our semi-coherent (differential) and non-coherent demodulators in the presence and absence of timing offsets/errors. When perfect timing is available, the noncoherent demodulator simplifies to a differential one (dashed curve). However, such a simplified differential receiver is essentially not operational if no timing synchronization is performed, as shown in Fig. 3 (star markers). In this case, the application of our noncoherent demodulator considerably reduces the BER level (triangle markers). With as few as 4 training symbols and a coarse synchronization step, the noncoherent demodulator brings the BER curve (diamond markers) to less than 2dB from the perfect timing case. Although some BER degradation is still present compared to the perfect timing case, the latter typically requires excess energy, bandwidth or processing complexity.

5. CONCLUSIONS

In this paper, we developed a noncoherent demodulator for UWB communications using PPM. Our demodulator consists of several novel elements including a differential encoder, a correlator using *modified* "dirty" templates and special signal processing which makes MLSD feasible. All these elements are tailored for PPM-UWB signals. The BER performance of our noncoherent demodulator is simulated with various timing conditions. The simulations show that our demodulator remains operational even when no synchronization is performed, and its performance in the presence of timing offset is less than 2dB away from the case with perfect timing.

6. REFERENCES

[1] R. Blazquez, P. Newaskar, and A. Chandrakasan, "Coarse acquisition for ultra wideband digital receivers," in *Proc. of ICASSP*, Apr. 6-10, 2003, pp. 137–40.

[2] J. D. Choi and W. E. Stark, "Performance of Ultra-Wideband communications with suboptimal receivers in multipath channels," *IEEE JSAC*, 20(9), pp. 1754–66, Dec. 2002.

[3] J. R. Foerster, *Channel Modeling Sub-committee Report Final*, IEEE P802.15-02/368r5-SG3a, IEEE P802.15 Working Group for WPAN, Nov. 2002.

[4] N. He and C. Tepedelenlioglu, "Analysis of a synchronization algorithm for non-coherent UWB receivers," in *Proc. of ICASSP*, Mar. 18-23, 2005, pp. 617 –20.

[5] M. Ho, V. Somayazulu, J. Foerster, and S. Roy, "A differential detector for an Ultra-Wideband communications system," in *Proc. of VVTC*, May 4-9, 2002, pp. 1896–900.

[6] R. T. Hoctor and H. W. Tomlinson, "Delay-hopped transmitted-reference RF communications," in *Proc. of UWBST*, May 20-23, 2002, pp. 265–9.

[7] B. M. Sadler and A. Swami, "On the performance of UWB and DS-spread spectrum communication systems," in *Proc. of UWBST*, May 20-23, 2002, pp. 289–92.

[8] R. A. Scholtz, "Multiple access with time-hopping impulse modulation," in *Proc. of MILCOM*, Oct. 11-14, 1993, pp. 447–50.

[9] D.-S. Shiu and J. M. Kahn, "Differential pulse-position modulation for power-efficient optical communication," *IEEE Trans. on Comm.*, 47(8), pp. 1201–10, Aug. 1999.

[10] Z. Tian and G. B. Giannakis, "Data-aided ML timing acquisition in Ultra-Wideband radios," in *Proc. of UWBST*, Nov. 16-19, 2003, pp. 142–6.

[11] M. Z. Win, G. Chrisikos, and N. R. Sollenberger, "Performance of rake reception in dense multipath channels: implications of spreading bandwidth and selection diversity order," *IEEE JSAC*, 18(58), pp. 1516–25, Aug. 2000.

[12] L. Yang, "Rapid and robust synchronization of PPM-UWB signals," in *Proc. of CISS*, Mar. 16-29, 2005.

[13] L. Yang and G. B. Giannakis, "Optimal pilot waveform assisted modulation for Ultra-Wideband communications," *IEEE Trans. on Wireless Comm.*, 3(4), pp. 1236–49, Jul. 2004.

[14] ——, "Ultra-wideband communications: An idea whose time has come," *IEEE SP Mag.*, 21(6), pp. 26–54, Nov. 2004.

[15] L. Yang, G. B. Giannakis, and A. Swami, "Noncoherent Ultra-Wideband radios," in *Proc. of MILCOM*, Oct. 31-Nov. 3, 2004.

[16] H. Zhang and D. L. Goeckel, "Generalized transmitted-reference UWB systems," in *Proc. of UWBST*, Nov. 16-19, 2003, pp. 147–51.

[17] D. Zwillinger, "Differential PPM has a higher throughput than PPM for band-limited and average-power-limited optical channel," *IEEE Trans. on Info. Th.*, 34(5), pp. 1269–73, Sep. 1988.